Isotopic composition of stratospheric ozone

Mao-Chang Liang,[1] Fredrick W. Irion,[2] Jason D. Weibel,[1] Charles E. Miller,[2]
Geoffrey A. Blake,[1] and Yuk L. Yung[1]

Received 8 June 2005; revised 23 September 2005; accepted 24 October 2005; published 18 January 2006.

[1] We present a kinetic calculation for the isotopic composition of stratospheric ozone. The calculated enrichments of $^{49}O_3$ and $^{50}O_3$ are in agreement with atmospheric measurements made at midlatitudes. Integrating the kinetic fractionation processes in the formation and photolysis of ozone, we obtain enrichments of ~7.5–10.5 and ~7.5–12.5% (referenced to atmospheric O_2) for $\delta^{49}O_3$ and $\delta^{50}O_3$, respectively, at altitudes between 20 and 35 km; the photolysis in the Hartley band of ozone is responsible for the observed altitude variation. The overall magnitude of the ozone enrichments (~10%) is large compared with that commonly known in atmospheric chemistry and geochemistry. The heavy oxygen atom in ozone is therefore useful as a tracer of chemical species and pathways that involve ozone or its derived products. For example, the mass anomalies of oxygen in two greenhouse gases, CO_2 and N_2O, are likely the consequences of the transfer of heavy oxygen atoms from ozone.

Citation: Liang, M.-C., F. W. Irion, J. D. Weibel, C. E. Miller, G. A. Blake, and Y. L. Yung (2006), Isotopic composition of stratospheric ozone, *J. Geophys. Res.*, *111*, D02302, doi:10.1029/2005JD006342.

1. Introduction

[2] It has been more than 20 years since the discovery of the heavy ozone anomaly [*Mauersberger*, 1981; *Thiemens and Heidenreich*, 1983]. The overall magnitude of the ozone enrichments is large compared with that commonly known in atmospheric chemistry and geochemistry. The heavy oxygen atom in ozone is therefore useful as a tracer of chemical species and pathways that involve ozone or its derived products. A quantitative analysis of the isotopic compositions in stratospheric ozone constitutes the main body of this paper. The enrichment, δ, is defined by

$$\delta(\%) = 100 \times \left(\frac{R_{smp}}{R_{std}} - 1\right), \tag{1}$$

where R_{smp} is the ratio of the abundances of an isotopically substituted species and its normal molecule and R_{std} is the same ratio in a standard sample. In this paper, the species of interest are ozone and atomic and molecular oxygen. Since molecular oxygen is the largest oxygen reservoir in the atmosphere and its isotopic composition is very stable, we choose the oxygen isotopic composition in atmospheric O_2 as our standard, rather than the more commonly employed V-SMOW (Vienna Standard Mean Ocean Water). The magnitudes of the atmospheric $\delta^{16}O^{17}O$ and $\delta^{16}O^{18}O$ are 1.175 and 2.35% referenced to V-SMOW, respectively, while the values are zero as referenced to O_2 itself.

[3] For simplicity, we define O = ^{16}O, P = ^{17}O, and Q = ^{18}O. Thus OOP, OPO, OOQ, and OQO represent $^{16}O^{16}O^{17}O$, $^{16}O^{17}O^{16}O$, $^{16}O^{16}O^{18}O$, and $^{16}O^{18}O^{16}O$, respectively. The doubly isotope substituted molecules are of negligible importance for the purposes of this paper, and $^{50}O_3$ is therefore primarily OOQ and OQO. In the stratosphere, the chemistry is governed primarily by the Chapman reactions:

$$O_2 + h\nu \rightarrow O + O \tag{2}$$

$$O + O_2 + M \rightarrow O_3 + M \tag{3}$$

$$O_3 + h\nu \rightarrow O_2 + O \tag{4}$$

$$O_3 + O \rightarrow O_2 + O_2 \tag{5}$$

$$O + O + M \rightarrow O_2 + M. \tag{6}$$

It has been known that equations (3) and (4) can result in noticeable ozone isotopic fractionation [*Gao and Marcus*, 2001; *Liang et al.*, 2004].

[4] Using a balloon-borne mass spectrometer, *Mauersberger* [1981] reports stratospheric enrichments of 0–40% in $^{50}O_3$, with a broad maximum between 28 and 38 km and a minimum at 20 km. The error was 15% at 30 km, increasing above and below that altitude. Recently, Mauersberger and colleagues acquired new data with the error lowered to ~5% [*Schueler et al.*, 1990; *Krankowsky et al.*, 2000; *Mauersberger et al.*, 2001; *Lämmerzahl et al.*, 2002] from ten balloon flights with more than 40 samples.

[1] Division of Geological and Planetary Sciences, California Institute of Technology, Pasadena, California, USA.
[2] Jet Propulsion Laboratory, California Institute of Technology, Pasadena, California, USA.

0148-0227/06/2005JD006342

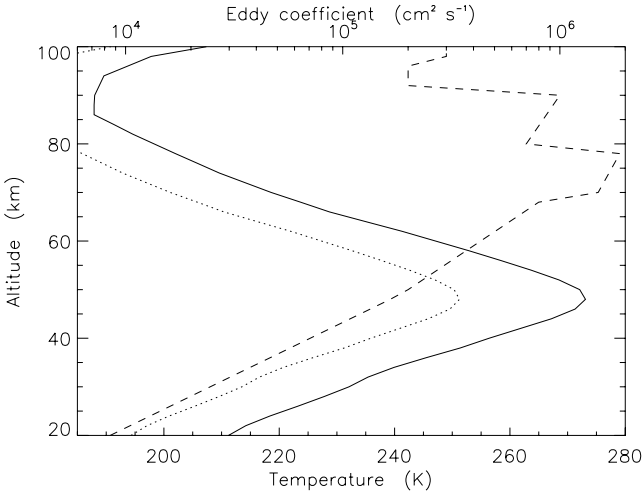

Figure 1. Profiles of temperature (solid line) and eddy diffusion coefficient (dashed line) used in the calculation. These two profiles are taken from *Allen et al.* [1981]. Dotted line represents a temperature profile equal to the solid line reduced by 8%.

The measured magnitude of the enrichments of ozone is ~10%, a value consistent with that obtained from ground-based and space-based Fourier transform infrared spectrometers (FTIR) [*Irion et al.*, 1996; *Meier and Notholt*, 1996]. Experimentally, *Thiemens and Heidenreich* [1983] first discovered that the formation of O_3 follows a slope of ~1 in three-isotope plots of ozone, instead of the typical ~0.5 dependence. Subsequent measurements demonstrated that the three-body reaction between O and O_2 (equation (3)) in their electronic ground states results in large enrichments for the heavier isotopologues [*Morton et al.*, 1990]. Later isotope specific reaction measurements further showed that the interaction channels to form asymmetric isotopomers are the major players in explaining the ozone isotopic anomaly [*Janssen et al.*, 1999, 2001, 2003; *Mauersberger et al.*, 1999].

[5] At room temperature, the measured enrichments of $^{49}O_3$ and $^{50}O_3$ in the production of ozone (equation (3)) are ~11 and 13%, respectively [*Thiemens and Heidenreich*, 1983; *Heidenreich and Thiemens*, 1985; *Thiemens and Jackson*, 1988; *Morton et al.*, 1990; *Anderson et al.*, 1997; *Mauersberger et al.*, 1999; *Janssen et al.*, 1999; *Janssen et al.*, 2003]. This result is by far the largest fractionation known in atmospheric chemistry and geochemistry and is in apparent contradiction to typical formation processes, in which the heavier molecules are depleted [e.g., *Kaye and Strobel*, 1983]. Recently, the introduction of the symmetry factor η has successfully explained this phenomenon as observed in the laboratory [*Hathorn and Marcus*, 1999, 2000; *Gao and Marcus*, 2001, 2002; *Gao et al.*, 2002], where η is applied to parameterize the deviation of the statistical density of states for symmetric isotopomers compared with asymmetric isotopomers. However, no quantitative atmospheric models including these formation processes, nor their impact on the isotopic composition of other species, have been reported.

[6] With newly available high-resolution measurements of ozone isotopic composition made at midlatitudes, it is found that the magnitude of the enrichments increases with altitude [*Krankowsky et al.*, 2000; *Mauersberger et al.*, 2001; *Lämmerzahl et al.*, 2002]. Mauersberger and colleagues [e.g., *Mauersberger et al.*, 2001] attempted to explain the altitude variation of the enrichments by temperature variation. The inferred temperature range at altitudes between ~20 and 35 km is ~200–260 K, which is much warmer than what is generally expected in the stratosphere for these latitudes and seasons, ~210–230 K.

[7] In general, the temperature gradient in the stratosphere is about 1 K km^{-1}. If the observed enrichment variation of heavy ozone is due entirely to the temperature variation in the stratosphere, the required temperature gradient is ~5 K km^{-1} on the basis of the averaged variation of enrichments with temperature of 0.06% K^{-1} measured in the laboratory [*Morton et al.*, 1990]. Therefore a process other than the temperature gradient is needed to account for this variation. It has been shown by *Bhattacharya et al.* [2002] that the photolysis-induced fractionation (equation (4)) at low pressures, such as those in the stratosphere, can result in high enrichment. In their paper, they defined a turnover time $\tau = [O_3]/[O_3]'$, where $[O_3]$ is the ozone density at a given time t and $[O_3]' = d[O_3]/dt$ is the corresponding dissociation rate, to explain this additional fractionation. With this turnover time, Bhattacharya et al. were able to reproduce the altitude variations of the enrichments of heavy ozone and predicted an enrichment of about 14% at 40 km. Instead of applying this artificial turnover time, we use the dissociation cross sections for isotopic substituted species calculated by the method described previously [*Blake et al.*, 2003; *Liang et al.*, 2004; *Miller et al.*, 2005].

[8] This paper is organized as follows. We describe the basics of the model incorporating the ozone enrichments from both formation and photolysis processes in section 2. The kinetic study for isotopically substituted ozone in the stratosphere is computed using the Caltech/JPL KINETICS one-dimensional diffusive chemical model. A detailed analysis of the model results and their comparison with atmospheric measurements is presented in section 3.

2. Atmospheric Models

2.1. One-Dimensional Model

[9] The one-dimensional Caltech/JPL KINETICS model is used in our study. A detailed description of the model has been given previously [e.g., *Allen et al.*, 1981]. Here, we summarize the most essential features only. The atmosphere is assumed to be in hydrostatic equilibrium, and the mass continuity equation is solved:

$$\frac{\partial n_i}{\partial t} + \frac{\partial \varphi_i}{\partial z} = P_i - L_i, \tag{7}$$

where n_i is the number density of species i, φ_i the transport flux, P_i the chemical production rate, and L_i the chemical loss rate, all evaluated at time t and altitude z. We are interested in a steady state solution, i.e., $\langle \partial n_i/\partial t \rangle \rightarrow 0$, in a diurnally averaged model. For the Earth's atmosphere, the homopause is located at 100 km above the surface, while the region of interest is well below it, i.e., altitudes $\lesssim$60 km. Eddy mixing is therefore the dominant term in φ_i. The profiles of temperature and eddy diffusion coefficients

Table 1. List of Chemical Reactions[a]

	Reactant(s)	Product(s)	Rate Coefficient	Notes and References[b]
(R1)	O_3+ hν	→ $O_2(^1\Delta_g)$ + $O(^1D)$	$J_1 = 4.21 \times 10^{-3}$	1, 5, 6, 14–17
(R2)		→ O_2+ O	$J_2 = 3.84 \times 10^{-4}$	1, 5, 6, 14–17
(R3)	OPO + hν	→ $OP(^1\Delta_g)$ + $O(^1D)$	$\approx J_1$	calculated; Figure 5
(R4)		→ OP + O	$\approx J_2$	calculated; Figure 6
(R5)	OOP + hν	→ $O_2(^1\Delta_g)$ + $P(^1D)$	$\approx \frac{1}{2}J_1$	calculated; Figure 5
(R6)		→ O_2+ P	$\approx \frac{1}{2}J_2$	calculated; Figure 6
(R7)		→ $OP(^1\Delta_g)$ + $O(^1D)$	$= J_5 \approx \frac{1}{2}J_1$	calculated; Figure 5
(R8)		→ OP + O	$= J_6 \approx \frac{1}{2}J_2$	calculated; Figure 6
(R9)	OQO + hν	→ $OQ(^1\Delta_g)$ + $O(^1D)$	$\approx J_1$	calculated; Figure 5
(R10)		→ OQ + O	$\approx J_2$	calculated; Figure 6
(R11)	OOQ + hν	→ $O_2(^1\Delta_g)$ + $Q(^1D)$	$\approx \frac{1}{2}J_1$	calculated; Figure 5
(R12)		→ O_2+ Q	$\approx \frac{1}{2}J_2$	calculated; Figure 6
(R13)		→ $OQ(^1\Delta_g)$ + $O(^1D)$	$= J_{11} \approx \frac{1}{2}J_1$	calculated; Figure 5
(R14)		→ OQ + O	$= J_{12} \approx \frac{1}{2}J_2$	calculated; Figure 6
(R15)	O_2+ hν	→ 2O	$J_{15} = 1.42 \times 10^{-7}$	1, 8, 9, 11, 18
(R16)	OP + hν	→ O + P	$= J_{15}$	assumed
(R17)	OQ + hν	→ O + Q	$= J_{15}$	assumed
(R18)	O_2+ hν	→ O + $O(^1D)$	$J_{18} = 6.50 \times 10^{-7}$	1, 8, 9, 11, 18
(R19)	OP + hν	→ $O(^1D)$ + P	$= \frac{1}{2}J_{18}$	assumed
(R20)		→ O + $P(^1D)$	$= \frac{1}{2}J_{18}$	assumed
(R21)	OQ + hν	→ $O(^1D)$ + Q =	$= \frac{1}{2}J_{18}$	assumed
(R22)		→ O + $Q(^1D)$	$= \frac{1}{2}J_{18}$	assumed
(R23)	O + O_2+ M	→ O_3+ M	$k_{23} = 1.76 \times 10^{-27}\ T^{-2.6}$	7
(R24)	O + OP + M	→ OOP + M	$\approx \frac{1}{2}k_{23}$	calculated; Figure 3
(R25)	O + OP + M	→ OPO + M	$\approx \frac{1}{2}k_{23}$	calculated; Figure 3
(R26)	O + OQ + M	→ OOQ + M	$\approx \frac{1}{2}k_{23}$	calculated; Figure 3
(R27)	O + OQ + M	→ OQO + M	$\approx \frac{1}{2}k_{23}$	calculated; Figure 3
(R28)	P + O_2+ M	→ OOP + M	$\approx k_{23}$	calculated; Figure 3
(R29)	Q + O_2+ M	→ OOQ + M	$\approx k_{23}$	calculated; Figure 3
(R30)	O + OP	→ P + O_2	$\approx \frac{1}{2}k_{33}$	calculated; Figure 3
(R31)	P + O_2	→ OP + O	$\approx k_{33}$	calculated; Figure 3
(R32)	O + OQ	→ Q + O_2	$\approx \frac{1}{2}k_{33}$	calculated; Figure 3
(R33)	Q + O_2	→ OQ + O	$k_{33} = 2.01 \times 10^{-10}\ T^{-0.9}$	2
(R34)	O + O_3	→ 2O_2	$k_{34} = 8.00 \times 10^{-12}\ e^{-2060/T}$	12
(R35)	O + OOP	→ OP + O_2	$= k_{34}$	assumed
(R36)	O + OPO	→ OP + O_2	$= k_{34}$	assumed
(R37)	O + OOQ	→ OQ + O_2	$= k_{34}$	assumed
(R38)	O + OQO	→ OQ + O_2	$= k_{34}$	assumed
(R39)	P + O_3	→ OP + O_2	$= k_{34}$	assumed
(R40)	Q + O_3	→ OQ + O_2	$= k_{34}$	assumed
(R50)	$O(^1D)$ + N_2	→ O + N_2	$k_{50} = 1.80 \times 10^{-11}\ e^{110/T}$	12
(R51)	$P(^1D)$ + N_2	→ P + N_2	$= k_{50}$	assumed
(R52)	$Q(^1D)$ + N_2	→ Q + N_2	$= k_{50}$	assumed
(R53)	$O(^1D)$ + O_2	→ O + O_2	$k_{53} = 3.20 \times 10^{-11}\ e^{70/T}$	12
(R54)	$P(^1D)$ + O_2	→ P + O_2	$= k_{53}$	assumed
(R55)	$Q(^1D)$ + O_2	→ Q + O_2	$= k_{53}$	assumed
(R56)[c]	$O_2(^1\Delta_g)$	→ O_2	$k_{56} = 2.58 \times 10^{-4}$	4, 13
(R57)[c]	$OP(^1\Delta_g)$	→ OP	$= k_{56}$	assumed
(R58)[c]	$OQ(^1\Delta_g)$	→ OQ	$= k_{56}$	assumed
(R59)	$O_2(^1\Delta_g)$ + O_2	→ O_2+ O_2	$k_{59} = 3.60 \times 10^{-18}\ e^{-200/T}$	12
(R60)	$OP(^1\Delta_g)$ + O_2	→ OP + O_2	$= k_{59}$	assumed
(R61)	$OQ(^1\Delta_g)$ + O_2	→ OQ + O_2	$= k_{59}$	assumed
(R62)	O + O + M	→ O_2+ M	$k_{62} = 4.30 \times 10^{-28}\ T^{-2}$	3
(R63)	O + P + M	→ OP + M	$= k_{62}$	assumed
(R64)	O + Q + M	→ OQ + M	$= k_{62}$	assumed
(R83)	O_3+ X	→ PROD + X	k_{83}	calculated; Figure 2
(R84)	OPO + X	→ PROD + X	$= k_{83}$	assumed
(R85)	OOP + X	→ PROD + X	$= k_{83}$	assumed
(R86)	OQO + X	→ PROD + X	$= k_{83}$	assumed
(R87)	OOQ + X	→ PROD + X	$= k_{83}$	assumed

[a]Electronic configurations are not shown for those atoms/molecules at their ground states. Units are s^{-1} for photolysis reactions, $cm^3\ s^{-1}$ for two-body reactions, and $cm^6\ cm^{-1}$ for three-body reactions. The photolysis rate coefficients are given at the top of the model atmosphere. Note that O = ^{16}O, P = ^{17}O, and Q = ^{18}O. (R83)–(R87) denote a net loss of ozone by catalysis (see text for details).

[b]References: 1, *Anbar et al.* [1993]; 2, *Anderson et al.* [1985]; 3, *Arnold and Comes* [1979]; 4, *Badger et al.* [1965]; 5, *Brock and Watson* [1980]; 6, *Fairchild et al.* [1978]; 7, *Hippler et al.* [1990]; 8, *Lee et al.* [1977]; 9, *Nicolet* [1984]; 10, *Parisse et al.* [1996]; 11, *Samson et al.* [1982]; 12, *Sander et al.* [2003]; 13, *Sandor et al.* [1997]; 14, *Sparks et al.* [1980]; 15, *Taherian and Slanger* [1985]; 16, *Turnipseed et al.* [1991]; 17, *Wine and Ravishankara* [1982]; 18, *Yung et al.* [1988].

[c]Spontaneous decay of excited O_2.

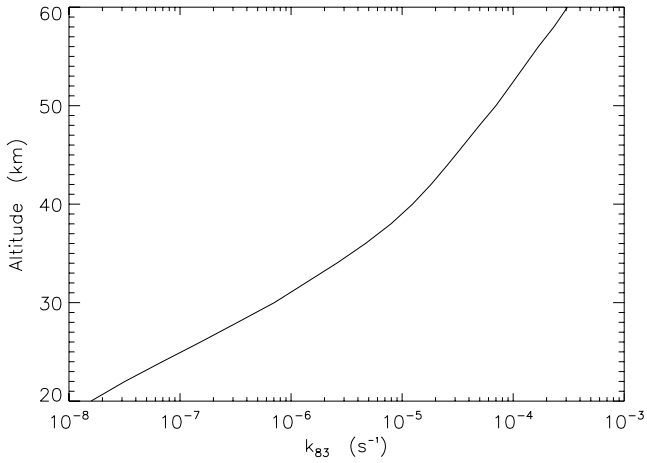

Figure 2. Profile of rate coefficient k_{83}, which is used to account for the net loss of ozone by catalysis in the stratosphere. See text for details.

are taken from *Allen et al.* [1981] and are reproduced in Figure 1.

[10] The model atmosphere consists of 66 layers evenly distributed from the surface to 130 km. Since the stratosphere is the region of principal interest, the chemistry is governed mainly by the Chapman reactions (equations (2)–(6)). Table 1 lists the reactions and rate coefficients used in this study. The reaction O_3+ X → PROD + X (R83) and its isotopic variants ((R84)–(R87)) simulate the net loss of ozone by NO_x, HO_x, and ClO_x catalysts. 'X' simply denotes that the reaction is catalyzed. The catalytic processes will drive the decomposition of ozone to O_2. Since O_2 is the largest oxygen reservoir, we do not trace the catalyzed products. The rate coefficients are assumed to be isotopically invariant and are calculated from the following five reactions:

$$NO_2 + O \rightarrow NO + O_2$$
$$OH + O \rightarrow H + O_2$$
$$HO_2 + O \rightarrow OH + O_2$$
$$HO_2 + O_3 \rightarrow OH + 2O_2$$
$$ClO + O \rightarrow Cl + O_2.$$

We obtain the reaction rates from a complete version of oxygen chemistry model in the stratosphere [*Jiang et al.*, 2004; *Morgan et al.*, 2004], multiply by 2, and then divide by the O_3 concentrations in that model. The factor of 2 indicates that either O or O_3 loss will eventually lead to the loss of ozone. The sum of the products for the above five reactions is used as the rate coefficient in (R83)–(R87) and shown in Figure 2. With these catalytic reactions, the resulting O_3 profiles within the simplified chemistry are in good agreement with that obtained by complete chemical models.

[11] When we switch off the fractionation in the rate coefficients in Table 1, the enrichments of O and O_3 relative to O_2 vanish, as expected, while $O(^1D)$ has a finite value of $\sim -0.5\%$. This deviation is a consequence of the nonnegligible abundances of OP and OQ. The abundances of OP and OQ relative to O_2 in the Earth's atmosphere are $\sim 8 \times 10^{-4}$ and 4×10^{-3}, respectively. The typical definition of isotopic compositions of $O(^1D)$ assumes that $O(^1D)$ is the derivative of O_3 only [see, e.g., *Yung et al.*, 1997]. However, $O(^1D)$ can also be produced from the photolysis of OPO, OOP, OQO, OOQ ((R3), (R7), (R9), (R13)). It turns out that

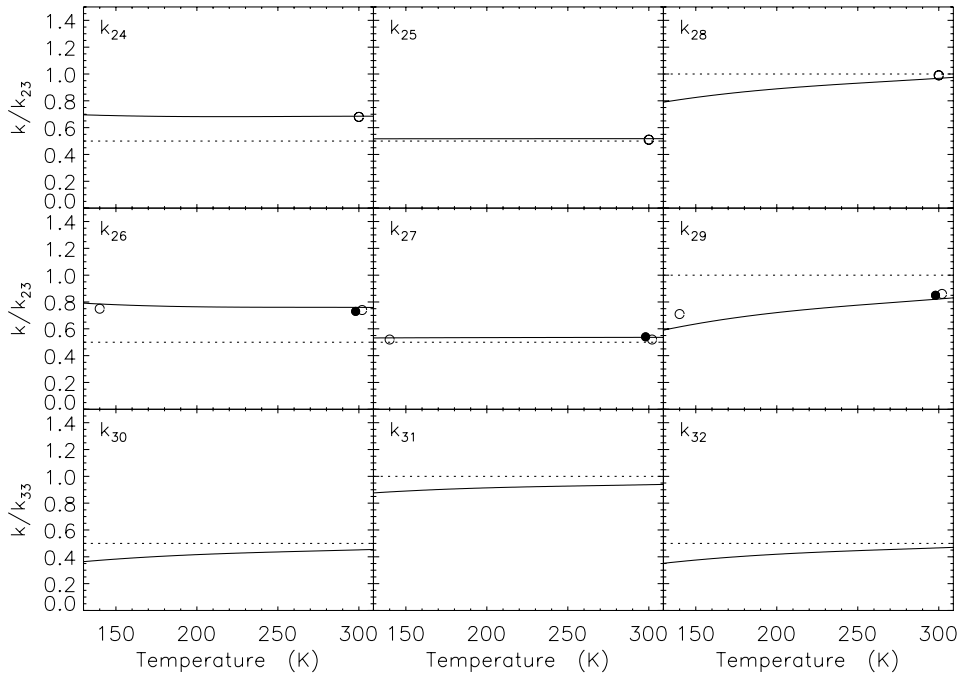

Figure 3. Calculated ozone formation and oxygen exchange rate coefficients (solid lines). Null fractionation is shown by dotted lines for reference. The solid circles are laboratory measurements of *Mauersberger et al.* [1999] and *Janssen et al.* [1999]. The open circles are from the calculation by *Gao and Marcus* [2002].

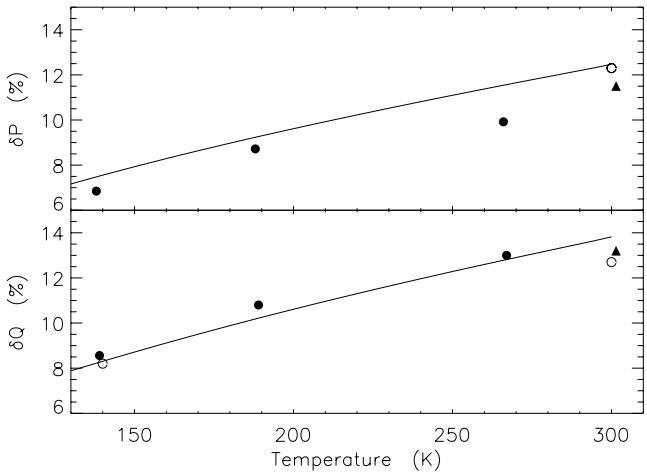

Figure 4. Enrichments resulting from the formation processes. Solid symbols are laboratory measurements: Circles were measured by *Morton et al.* [1990], and triangles were measured by *Mauersberger et al.* [1999]. The open circles were calculated by *Gao and Marcus* [2002].

the abundances of OP and OQ determine the enrichment of $O(^1D)$. The $\sim -0.5\%$ value is simply $-(8 \times 10^{-4} + 4 \times 10^{-3})$.

2.2. Ozone Formation

[12] We follow Gao and Marcus' approach to calculate the rate coefficients relevant to our study [*Gao and Marcus*, 2001, 2002]. Since the pressure of interest is less than 50 mbar (altitudes greater than 20 km), the formation rates of ozone are close to their low-pressure limit, that is, the pressure dependence is insignificant; the difference of enrichments for heavier ozone is <0.5% between 10 and 50 mbar [see, e.g., *Morton et al.*, 1990]. It is also because of the low pressure in the region of interest that the coefficient can be well calculated by the free-rotor model (see *Gao and Marcus* [2002] for details), in which the interaction between atomic and molecular oxygen is simplified. Hence, for simplicity, we calculate the rate coefficients using a free-rotor approach.

[13] It is important to note that the production rate of asymmetric molecules is not simply the sum of the rate coefficients of two reactive channels measured in the laboratory or calculated in the theory. For example, the products of OOQ and QOO are the results of two different reaction channels:

$$\mathrm{O + OQ + M \rightarrow OOQ + M}$$
$$\mathrm{Q + OO + M \rightarrow QOO + M.}$$

The fractionation in the production of OOQ is not the sum of the fractionations of the rate coefficients in the above two reactions. When there is rapid exchange reaction between atomic and molecular oxygen, one can multiply the second reaction by the equilibrium constant in the reaction $\mathrm{O + OQ \rightleftarrows Q + OO}$ [see, e.g., *Hathorn and Marcus*, 1999, (2.11)–(2.13); *Gao and Marcus*, 2002, (2.36)]. The product after multiplying by an additional factor of 2 is used in (R29) (and (R28) for OOP production) of Table 1. The factor 2 indicates that OOQ can be formed by attaching Q to OO from either side.

[14] The ozone layer is located mainly at altitudes between 20 and 50 km (50–1 mbar), and its mixing ratio peaks at ~30 km (~10 mbar). Because of the weak pressure dependence in the enrichments of ozone in the stratosphere, we calculate the rate coefficients of ozone production at 10 mbar where the mixing ratio of ozone peaks. The enrichment is rather sensitive to temperature, however. The variation of the enrichments from 140 to 300 K is about 4–5% in the low-pressure limit, or $\sim 0.03\%\ \mathrm{K}^{-1}$ (or $0.06\%\ \mathrm{K}^{-1}$ when incorporating $\mathrm{O + O_2}$ exchange reactions) [*Morton et al.*, 1990].

[15] The parameters η and ΔE are taken to be the same as those suggested by *Gao and Marcus* [2001], that is, η = 1.13 at 140 K and 1.18 at 300 K and we use linear interpolation in between, and $\Delta E = 260\ \mathrm{cm}^{-1}$. The reaction rate coefficients are calculated and shown in Figure 3, along with laboratory measurements and theoretical calculations. The exchange rate coefficients of O and O_2 are given in the lowermost panels. The dotted lines in Figure 3 represent the reference case in which the fractionation in the rate coefficients is removed. The calculated enrichments of ozone are plotted in Figure 4. The laboratory measurements [*Morton et al.*, 1990; *Mauersberger et al.*, 1999] and the published calculated values [*Gao and Marcus*, 2002] are

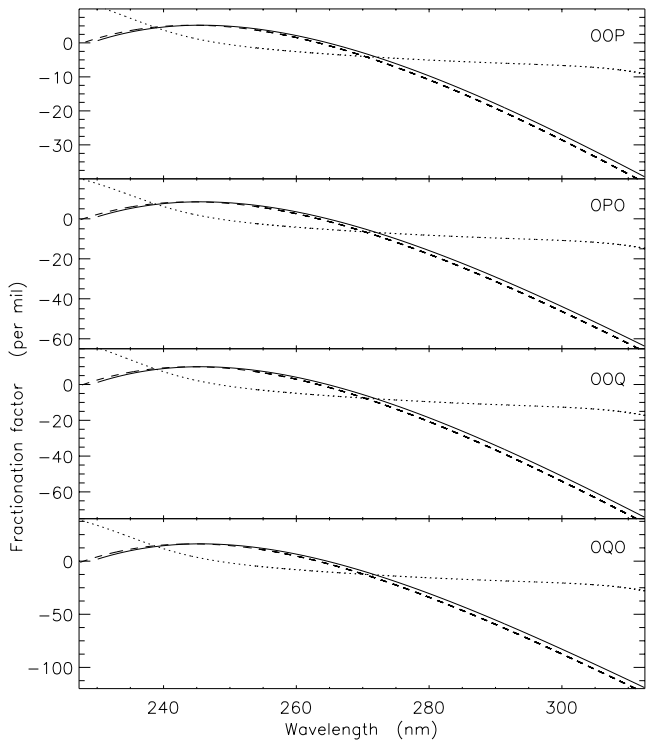

Figure 5. Fractionation factors calculated using the MZPE model in the Hartley band at 195 (dashed lines) and 295 K (solid lines). Results calculated using the *Yung and Miller* [1997] model are shown by dotted lines. The fractionation factor is defined by $1000 \times (\sigma/\sigma_0 - 1)$, where σ_0 and σ are the photoabsorption cross sections of normal and isotopically substituted molecules, respectively.

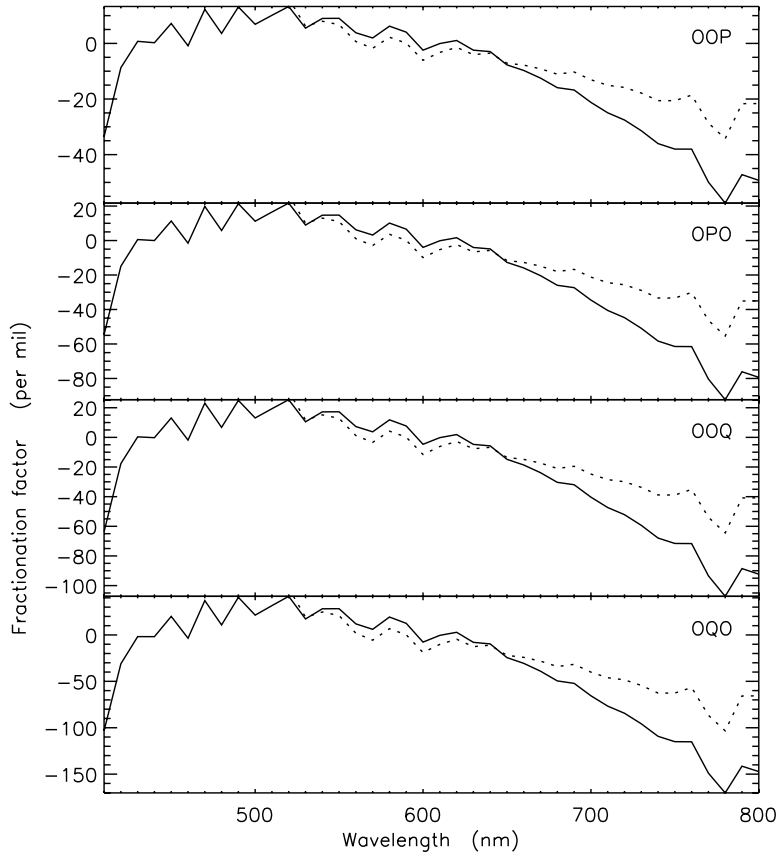

Figure 6. Fractionation factors calculated using the MZPE model in the Chappuis band at 295 K (solid lines). Results calculated using the *Yung and Miller* [1997] model are shown by dotted lines.

overplotted by filled and open symbols, respectively. We note that the calculation of δQ agrees with experiments better than that for δP. While the errors for δQ are ≲5%, the errors of δP can be as large as 50%. Further improvement in the theory of temperature-dependent and isotope-specific formation rates of ozone are therefore needed.

2.3. Ozone Photolysis

[16] The photoabsorption cross sections and photolysis quantum yields of OOP, OPO, OOQ, and OQO have not yet been measured. A zero point energy-based semianalytic model (MZPE model, hereafter) is applied to calculate the cross sections for the above species [*Blake et al.*, 2003; *Liang et al.*, 2004; *Miller et al.*, 2005]. In the Earth's atmosphere, the photolysis of ozone is primarily in the Hartley and Chappuis bands, where the latter dominates in the regions ≲35 km. The calculation in the Hartley band at room temperature was reported by *Liang et al.* [2004] and is reproduced here by the solid lines in Figure 5. We also perform the same calculation in the Chappuis band, and the results are shown in Figure 6.

[17] In each band, there are two channels for the dissociation of asymmetric molecules. For example in the Hartley band OOQ can be dissociated into either $O(^1D)$ + $OQ(^1\Delta_g)$ or $O_2(^1\Delta_g)$ + $Q(^1D)$. We assume these two branches are equally weighted. Whether this assumption is valid does not affect the results obtained in this paper. The robustness of this assumption arises from the fact that the abundance of ozone is negligible compared with that of molecular oxygen, and fast exchange reactions between atomic and molecular oxygen quickly wash out the isotopic fractionations in the photolytic products of ozone. However, the subsequent reactions involving $O(^1D)$ can be seriously modified by this assumption, but are beyond the scope of this paper. M.-C. Liang et al. (Oxygen isotopic composition of carbon dioxide in the middle atmosphere, submitted to *Proc. Natl. Acad. Sci.*, 2005, hereinafter referred to as Liang et al., submitted manuscript, 2005) will show that the assumption of equally weighted channels in the photolysis of ozone can explain the observed isotopic compositions of CO_2 in the middle atmosphere.

[18] Temperature variation may be a factor important to the photolysis-induced fractionation. For example, N_2O shows a nonnegligible temperature variation [e.g., *Liang et al.*, 2004]. To verify the sensitivity to temperature, we also calculate the fractionation of the cross sections of heavy ozone at 195 K. The absorption ozone cross section of normal ozone at 195 K was taken from *Freeman et al.* [1984] and *Yoshino et al.* [1988, 1993]. The results of the fractionation are shown by the dashed lines in Figure 5. Unlike N_2O, ozone shows a negligible temperature dependence, at least in the Hartley band. So, for simplicity, we ignore the temperature dependence of photoabsorption cross sections in our model.

[19] It has been shown that the ozone photodissociation in the Huggins band can result in fractionation as large as ∼30% [*Miller et al.*, 2005]. However, the process takes place at UV wavelengths longer than 300 nm, where the

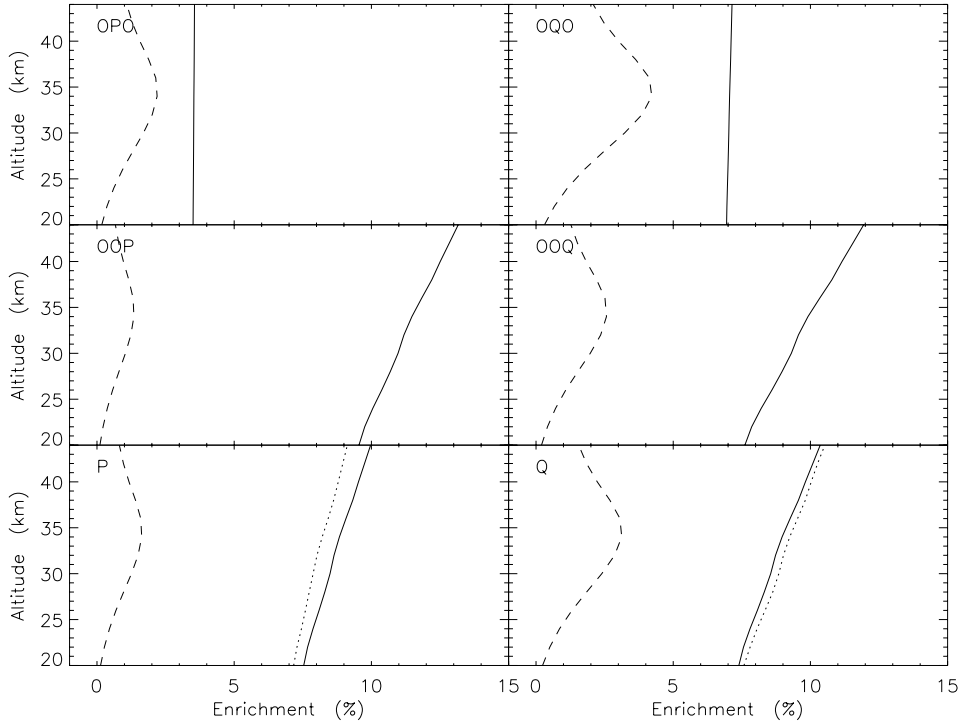

Figure 7. Enrichments for the species indicated in the top left corner of each plot. Enrichments calculated using the formation and photolysis models are shown by solid and dashed lines, respectively. The dotted lines are the laboratory measurements [*Morton et al.*, 1990].

cross section is small. The photodissociation coefficients in the Huggins band are orders of magnitude less than those in the Hartley and Chappuis bands. The overall contribution from this band is relatively small, and we ignore it in this paper.

3. Results

[20] Following equation (1), the enrichment of heavy ozone in this paper is defined by

$$\delta\mathrm{OQO}\ (\%) = 100 \times \left(\frac{2[\mathrm{OQO}/\mathrm{O_3}]}{[\mathrm{OQ}/\mathrm{O_2}]} - 1\right) \tag{8}$$

$$\delta\mathrm{OOQ}\ (\%) = 100 \times \left(\frac{[\mathrm{OOQ}/\mathrm{O_3}]}{[\mathrm{OQ}/\mathrm{O_2}]} - 1\right) \tag{9}$$

$$\delta\mathrm{Q}\ (\%) = (\delta\mathrm{OQO} + 2\delta\mathrm{OOQ})/3. \tag{10}$$

A similar definition holds for OPO and OOP, but with substitution of Q by P. Here, we assume conventional statistical weights for symmetric (OPO and OQO) and asymmetric (OOP and OOQ) molecules.

[21] In this paper, we concentrate on the stratosphere, where the diurnal temperature variation is small. In the troposphere near the surface, the overall δP and δQ are ∼6.5–8 and 8–9%, respectively [*Krankowsky et al.*, 1995; *Johnston and Thiemens*, 1997]. The measured variation of the enrichments of ozone is as large as ∼0.5%. The overall enrichments can roughly be explained by the formation at ∼300 K [*Morton et al.*, 1990]. With 0.06% K^{-1} temperature variations, the inferred temperature variation is ∼10 K.

3.1. Vertical Profiles

[22] Figures 7 and 8 show the calculated enrichments for ozone isotopomers and isotopologues. We see that the formation-induced enrichments alone can roughly explain the magnitude of the observed values. Figures 7 and 8 indicate that the enrichments due to the formation of symmetric molecules are about a factor of two smaller than those of asymmetric molecules, while the opposite is true for photolysis-induced enrichments. Enrichments resulting from photolysis are about an order of magnitude less than those from formation.

3.1.1. Formation

[23] The enrichments of symmetric molecules show little altitude dependence, while those for asymmetric molecules increase with altitude above ∼20 km (solid lines of Figure 7). For symmetric molecules (OPO and OQO), the enrichment gradients are negligible, $\lesssim$0.003% K^{-1}. For asymmetric molecules (OOP and OOQ), the gradients are a factor of about 20 greater, ∼0.06% K^{-1}, consistent with the laboratory measurements [*Morton et al.*, 1990]. The magnitudes of the enrichments for symmetric molecules are smaller than those for asymmetric molecules, and their abundance is also a factor of two less than that of asymmetric variants. Therefore the overall enrichments, as well as their temperature variations, are contributed primarily by asymmetric molecules. The dotted lines in the bottom two panels of Figure 7 represent laboratory measured enrichments for P and Q [*Morton et al.*, 1990]. The values are consistent with those in Figure 4.

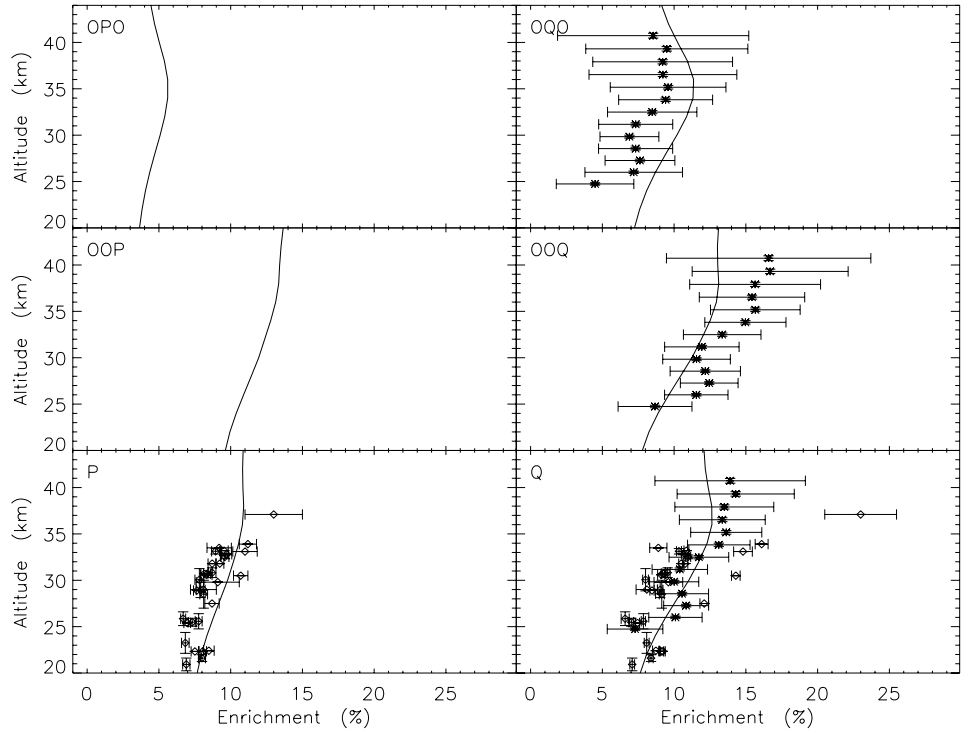

Figure 8. Total enrichments calculated by integrating the formation and photolysis models. The error bars in the atmospheric measurements are for 1σ. The diamonds are mass spectroscopic measurements [*Krankowsky et al.*, 2000; *Mauersberger et al.*, 2001; *Lämmerzahl et al.*, 2002], and asterisks are FTIR measurements by *Irion et al.* [1996].

3.1.2. Photolysis

[24] The enrichments of the isotopomers and isotopologues of ozone from photolysis are shown by the dashed lines in Figure 7. The enrichments peak at ∼35 km and are significant only at altitudes between 20 and 50 km, where the ozone layer peaks. The magnitude of the fractionation is sensitive to the wavelength of incident UV photons (see Figure 5). Therefore it is expected that the attenuation of UV radiation can result in large vertical variations of the enrichments. At high altitudes, the photolysis is primarily through photons at the maximum of the Hartley band, where the fractionation is small. Lower in the atmosphere, absorption in the long-wavelength wing of the Hartley band becomes important, and fractionation is large in this region. Below the ozone peak, photolysis in the Chappuis band dominates, and there is little fractionation (Figure 6).

3.1.3. Overall Enrichments

[25] The isotopic fractionation from both formation and photolysis are presented in Figure 8. We see that the combined enrichments better match the observations.

3.2. Three-Isotope Plots

[26] Figure 9 shows a three-isotope plot of ozone at altitudes between 20 and 35 km. The slope measured in the laboratory is ∼0.6 (dotted line), but the associated error is significant and the slope varies with temperature [see *Morton et al.*, 1990, Figure 3]. The slope for a linear least squares fit to the atmospheric measurements is ∼1. The slope in the formation processes in our model is ∼0.8, close to but not quite unity (solid line). The slope from the photolysis is mass-dependent, or ∼0.5 (inset).

[27] It is shown that the enrichment variations from formation are about 1.5% for δQ and about 1% for δP. The observations show a factor of ∼3 broader. If temperature variation is the key to the observed variation of the enrichments, the required variation is >60 K, an unreasonable value in the stratosphere. However, we show next that the photolysis-induced enrichments can account for these variations. As shown in the inset of Figure 9, the variations of δQ and δP are ∼3 and 1.5%, respectively.

[28] In the altitude range 22 to 33 km, the observed enrichments for P and Q are, respectively, ∼7–10 and ∼7–11%, while the calculated values are ∼8–10.5 and ∼8–12.5%. For OPO and OOP, the variations are ∼1.5 and ∼2.5%. For OQO and OOQ, they are ∼2 and ∼4%. It is important to note that the calculated overall enrichments are about 1–1.5% (dotted line of Figure 10) in excess of the measurements, suggesting that other processes, as important as photolysis, may be missing in our study.

[29] Since the photolysis lifetime of stratospheric ozone is only about one hour, the transport does little to change the vertical profiles of the enrichments. To lower the calculated values, we could reduce the effect from either formation or photolysis. For the formation channel, we show in Figure 10 that an 8% reduction (∼20 K) of temperature in our reference profile, shown by the dotted line in Figure 1, reproduces the observations well. From photolysis, we need to increase the ozone column above 40 km by a factor of >5, which can then move the peaks of the photolysis-induced enrichments upward by ∼5 km, thus reducing the enrichments in the regions between 20 and 35 km. However, both are unlikely, because the required modification in the

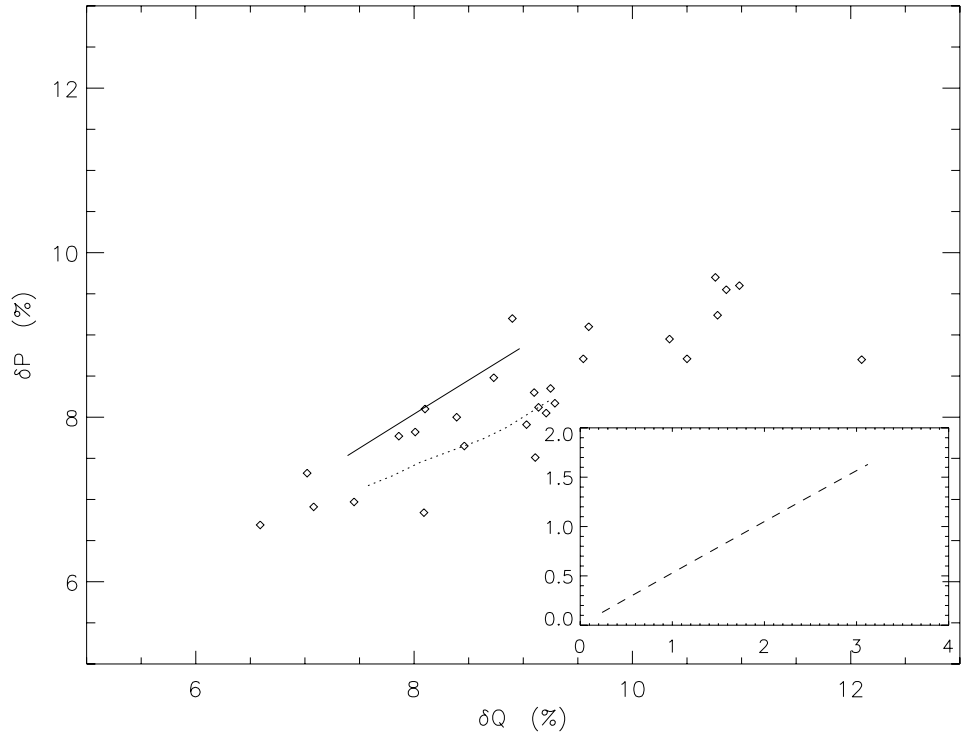

Figure 9. Three-isotope plot of ozone in the regions between 20 and 35 km. Diamonds are balloon-borne mass spectrometer measurements [*Krankowsky et al.*, 2000; *Mauersberger et al.*, 2001; *Lämmerzahl et al.*, 2002]. The solid and dashed lines are the calculated formation- and photolysis-induced enrichments, respectively. The dotted line is the laboratory measurements [*Morton et al.*, 1990].

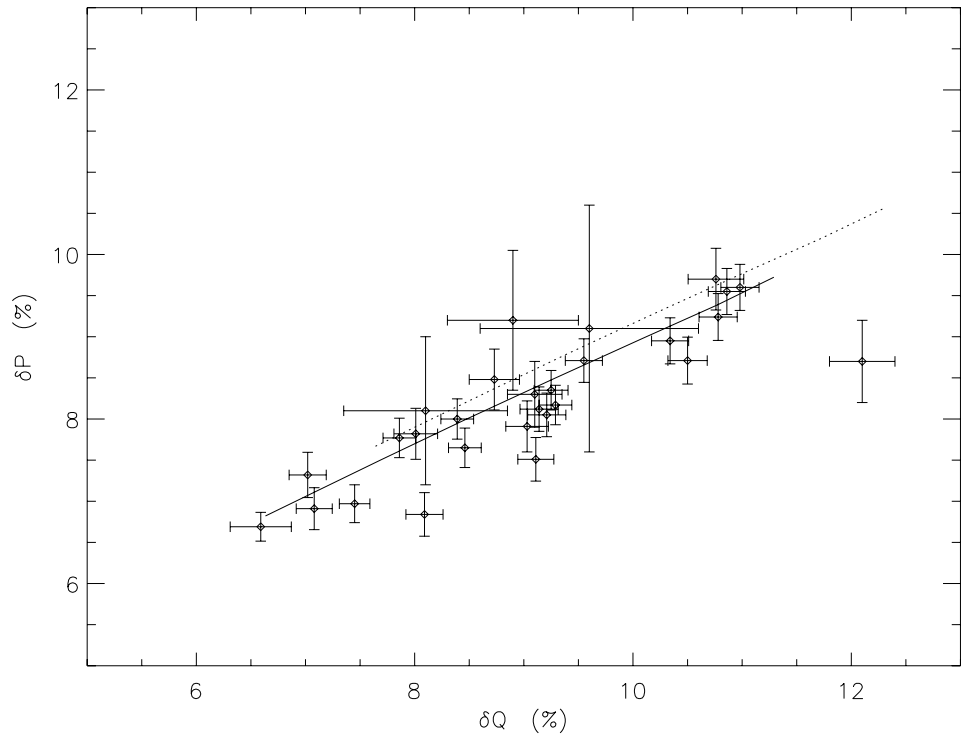

Figure 10. Three-isotope plot of ozone in the regions between 20 and 35 km, using the temperature profile shown by dotted line in Figure 1. Dotted line shows the profiles obtained using the reference temperature profile. The field measurements are symbolized (see the caption in Figure 9 for the references). One-σ error bars are overplotted.

temperature and ozone abundance in the stratosphere is beyond the uncertainties of the current knowledge of the stratosphere. More laboratory measurements on the formation and photolysis rate coefficients for ozone are urgently needed to refine our calculations.

4. Conclusion

[30] In this paper, we have modeled processes affecting the isotopic composition of heavy ozone in detail. The enrichments resulting from the formation processes, which are on the order of 10%, are by far the most significant in the known chemical and geochemical fractionation mechanism. At altitudes between 20 and 35 km, the enrichments for $^{49}O_3$ and $^{50}O_3$ are 7–9% and 7–11%, respectively. *Krankowsky et al.* [2000] and *Mauersberger et al.* [2001] attribute the altitude variation to the temperature variation in the stratosphere, and the estimated temperature ranges 200–260 K. However, the expected temperature in the stratosphere is between ~210 and 230 K. *Bhattacharya et al.* [2002] proposed that the ozone dissociation provides additional fractionation to the existing enrichments resulting from formation processes. They introduced an ad hoc parameter of turnover time to simulate the photodissociation-induced enrichments. With this turnover time, they were able to reproduce the observed altitude variations of the enrichments of heavy ozone.

[31] To avoid this artificial parameter, we use the calculated dissociation cross sections for isotopically substituted species. The cross sections are calculated by means of the MZPE model (see, e.g., *Liang et al.* [2004] for details). With this, we are able to calculate the enrichments of heavy ozone quantitatively. We perform a modeling study using one-dimensional Caltech/JPL KINETICS code which takes the optical depths from the molecular absorption (mainly oxygen and ozone in the stratosphere) properly into account. The altitude variation of heavy ozone enrichments is thereby reproduced. When incorporating this additional effect into the formation-induced enrichments, the overall values of the enrichments are systematically 1–1.5% in excess of the observation. With large modifications to the temperature profile (8% reduction) and ozone column (>5 times enhancement above 40 km) in the stratosphere, we would be able to reproduce the observations. It is also possible that we have overestimated the enrichments from photolysis, though the MZPE model calculation has successfully reproduced the laboratory measured cross section of $^{18}O^{18}O^{18}O$ [see *Liang et al.*, 2004, Figure 8]. A two-dimensional model, which determines the ozone abundances between latitudes more accurately, is needed to verify if the temperature profiles are responsible for this ~1% difference in the enrichments of stratospheric ozone.

[32] The enrichments of heavy ozone are the most prominent feature in the isotopic chemistry in the stratosphere. This large oxygen isotopic effect can be transferred to other long-lived molecules such as CO_2. Therefore their isotopic composition can be used to trace detailed chemical and dynamical processes in the stratosphere and mesosphere. A similar mechanism has been applied to CO_2 [e.g., *Yung et al.*, 1991, 1997], and the measured profile of $C^{16}O^{18}O$ is explained. *Barth and Zahn* [1997] extended this mechanism to $C^{16}O^{17}O$. They were able to calculate the observed slope of ~2 in three-isotope plots of oxygen in CO_2, though several assumptions must be made to reproduce this slope. Liang et al. (submitted manuscript, 2005) remove the assumptions by *Barth and Zahn* [1997] and successfully reproduce the slope of ~1.7 in the observed enrichments of CO_2.

[33] **Acknowledgments.** Special thanks to Yi-Qin Gao for helping us on the ozone formation model. We also thank Mimi Gerstell, Jack Margolis, Run-Lie Shia, and Geoff Toon for their helpful comments. This work was supported by an NSF grant ATM-9903790.

References

Allen, M., Y. L. Yung, and J. W. Waters (1981), Vertical transport and photochemistry in the terrestrial mesosphere and lower thermosphere (50–120 km), *J. Geophys. Res.*, *86*, 3617–3627.

Anbar, A. D., M. Allen, and H. A. Nair (1993), Photodissociation in the atmosphere of Mars: Impact of high-resolution, temperature-dependent CO_2 cross-section measurements, *J. Geophys. Res.*, *98*, 10,925–10,931.

Anderson, S. M., F. S. Klein, and F. Kaufman (1985), Kinetics of the isotope exchange-reaction of ^{18}O with NO and O_2 at 298-K, *J. Chem. Phys.*, *83*, 1648–1656.

Anderson, S. M., D. Hulsebusch, and K. Mauersberger (1997), Surprising rate coefficients for four isotopic variants of $O + O_2 + M$, *J. Chem. Phys.*, *107*, 5385–5392.

Arnold, I., and F. J. Comes (1979), Temperature-dependence of the reactions $O(^3P) + O_3 \Rightarrow 2O_2$ and $O(^3P) + O_2 + M \Rightarrow O_3 + M$, *Chem. Phys.*, *42*, 231–239.

Badger, R. M., A. C. Wright, and R. F. Whitlock (1965), Absolute intensities of discrete and continuous absorption bands of oxygen gas at 1.26 and 1.065 μm and radiative lifetime of $^1\Lambda_g$ state of oxygen, *J. Chem. Phys.*, *43*, 4345–4350.

Barth, V., and A. Zahn (1997), Oxygen isotope composition of carbon dioxide in the middle atmosphere, *J. Geophys. Res.*, *102*, 12,995–13,007.

Bhattacharya, S. K., S. Chakraborty, J. Savarino, and M. H. Thiemens (2002), Low-pressure dependency of the isotopic enrichment in ozone: Stratospheric implications, *J. Geophys. Res.*, *107*(D23), 4675, doi:10.1029/2002JD002508.

Blake, G. A., M. C. Liang, C. G. Morgan, and Y. L. Yung (2003), A Born-Oppenheimer photolysis model of N_2O fractionation, *Geophys. Res. Lett.*, *30*(12), 1656, doi:10.1029/2003GL016932.

Brock, J. C., and R. T. Watson (1980), Ozone photolysis—Determination of the $O(^3P)$ quantum yield at 266-nm, *Chem. Phys. Lett.*, *71*, 371–375.

Fairchild, C. E., E. J. Stone, and G. M. Lawrence (1978), Photofragment spectroscopy of ozone in UV region 270–310 nm and at 600 nm, *J. Chem. Phys.*, *69*, 3632–3638.

Freeman, D. E., K. Yoshino, J. R. Esmond, and W. H. Parkinson (1984), High-resolution absorption cross-section measurements of ozone at 195-K in the wavelength region 240–350 nm, *Planet. Space Sci.*, *32*, 239–248.

Gao, Y. Q., and R. A. Marcus (2001), Strange and unconventional isotope effects in ozone formation, *Science*, *293*, 259–263.

Gao, Y. Q., and R. A. Marcus (2002), On the theory of the strange and unconventional isotopic effects in ozone formation, *J. Chem. Phys.*, *116*, 137–154.

Gao, Y. Q., W. C. Chen, and R. A. Marcus (2002), A theoretical study of ozone isotopic effects using a modified ab initio potential energy surface, *J. Chem. Phys.*, *117*, 1536–1543.

Hathorn, B. C., and R. A. Marcus (1999), An intramolecular theory of the mass-independent isotope effect for ozone. I, *J. Chem. Phys.*, *111*, 4087–4100.

Hathorn, B. C., and R. A. Marcus (2000), An intramolecular theory of the mass-independent isotope effect for ozone. II. Numerical implementation at low pressures using a loose transition state, *J. Chem. Phys.*, *113*, 9497–9509.

Heidenreich, J. E., and M. H. Thiemens (1985), The non-mass-dependent oxygen isotope effect in the electrodissociation of carbon-dioxide—A step toward understanding nomad chemistry, *Geochim. Cosmochim. Acta*, *49*, 1303–1306.

Hippler, H., R. Rahn, and J. Troe (1990), Temperature and pressure-dependence of ozone formation rates in the range 1–1000-bar and 90–370-K, *J. Chem. Phys.*, *93*, 6560–6569.

Irion, F. W., M. R. Gunson, C. P. Rinsland, Y. L. Yung, M. C. Abrams, A. Y. Chang, and A. Goldman (1996), Heavy ozone enrichments from Atmos infrared solar spectra, *Geophys. Res. Lett.*, *23*, 2377–2380.

Janssen, C., J. Guenther, D. Krankowsky, and K. Mauersberger (1999), Relative formation rates of $^{50}O_3$ and $^{52}O_3$ in $^{16}O^{18}O$ mixtures, *J. Chem. Phys.*, *111*, 7179–7182.

Janssen, C., J. Guenther, K. Mauersberger, and D. Krankowsky (2001), Kinetic origin of the ozone isotope effect: A critical analysis of enrichments and rate coefficients, *Phys. Chem. Chem. Phys.*, *3*, 4718–4721.

Janssen, C., J. Guenther, D. Krankowsky, and K. Mauersberger (2003), Temperature dependence of ozone rate coefficients and isotopologue fractionation in ^{16}O-^{18}O oxygen mixtures, *Chem. Phys. Lett.*, *367*, 34–38.

Jiang, X., C. D. Camp, R. Shia, D. Noone, C. Walker, and Y. L. Yung (2004), Quasi-biennial oscillation and quasi-biennial oscillation-annual beat in the tropical total column ozone: A two-dimensional model simulation, *J. Geophys. Res.*, *109*, D16305, doi:10.1029/2003JD004377.

Johnston, J. C., and M. H. Thiemens (1997), The isotopic composition of tropospheric ozone in three environments, *J. Geophys. Res.*, *102*, 25,395–25,404.

Kaye, J. A., and D. F. Strobel (1983), Enhancement of heavy ozone in the Earth's atmosphere, *J. Geophys. Res.*, *88*, 8447–8452.

Krankowsky, D., F. Bartecki, G. G. Klees, K. Mauersberger, K. Schellenbach, and J. Stehr (1995), Measurement of heavy isotope enrichment in tropospheric ozone, *Geophys. Res. Lett.*, *22*, 1713–1716.

Krankowsky, D., P. Lämmerzahl, and K. Mauersberger (2000), Isotopic measurements of stratospheric ozone, *Geophys. Res. Lett.*, *27*, 2593–2595.

Lämmerzahl, P., T. Röckmann, C. A. M. Brenninkmeijer, D. Krankowsky, and K. Mauersberger (2002), Oxygen isotope composition of stratospheric carbon dioxide, *Geophys. Res. Lett.*, *29*(12), 1582, doi:10.1029/2001GL014343.

Lee, L. C., T. G. Slanger, G. Black, and R. L. Sharpless (1977), Quantum yields for production of O(1D) from photodissociation of O_2 at 1160–1770 Å, *J. Chem. Phys.*, *67*, 5602–5606.

Liang, M. C., G. A. Blake, and Y. L. Yung (2004), A semianalytic model for photo-induced isotopic fractionation in simple molecules, *J. Geophys. Res.*, *109*, D10308, doi:10.1029/2004JD004539.

Mauersberger, K. (1981), Measurement of heavy ozone in the stratosphere, *Geophys. Res. Lett.*, *8*, 935–937.

Mauersberger, K., B. Erbacher, D. Krankowsky, J. Gunther, and R. Nickel (1999), Ozone isotope enrichment: Isotopomer-specific rate coefficients, *Science*, *283*, 370–372.

Mauersberger, K., P. Lämmerzahl, and D. Krankowsky (2001), Stratospheric ozone isotope enrichments: Revisited, *Geophys. Res. Lett.*, *28*, 3155–3158.

Meier, A., and J. Notholt (1996), Determination of the isotopic abundances of heavy O3 as observed in Arctic ground-based FTIR-spectra, *Geophys. Res. Lett.*, *23*, 551–554.

Miller, C. E., R. M. Onorato, M.-C. Liang, and Y. L. Yung (2005), Extraordinary isotopic fractionation in ozone photolysis, *Geophys. Res. Lett.*, *32*, L14814, doi:10.1029/2005GL023160.

Morgan, C. G., M. Allen, M. C. Liang, R. L. Shia, G. A. Blake, and Y. L. Yung (2004), Isotopic fractionation of nitrous oxide in the stratosphere: Comparison between model and observations, *J. Geophys. Res.*, *109*, D04305, doi:10.1029/2003JD003402.

Morton, J., J. Barnes, B. Schueler, and K. Mauersberger (1990), Laboratory studies of heavy ozone, *J. Geophys. Res.*, *95*, 901–907.

Nicolet, M. (1984), On the molecular-scattering in the terrestrial atmosphere—An empirical-formula for its calculation in the homosphere, *Planet. Space Sci.*, *32*, 1467–1468.

Parisse, C., J. Brion, and J. Malicet (1996), UV absorption spectrum of ozone: Structure analysis and study of the isotope effect in the Hartley System, *Chem. Phys. Lett.*, *248*, 31–36.

Samson, J. A. R., G. H. Rayborn, and P. N. Pareek (1982), Dissociative photo-ionization cross-sections of O_2 from threshold to 120-Å, *J. Chem. Phys.*, *76*, 393–397.

Sander, S. P., et al. (2003), Chemical kinetics and photochemical data for use in atmospheric studies, *Eval. 14*, *JPL Publ. 02-25*, Jet Propul. Lab., Pasadena, Calif.

Sandor, B. J., R. T. Clancy, D. W. Rusch, C. E. Randall, R. S. Eckman, D. S. Siskind, and D. O. Muhleman (1997), Microwave observations and modeling of $O_2(^1\Delta_g)$ and O_3 diurnal variation in the mesosphere, *J. Geophys. Res.*, *102*, 9013–9028.

Schueler, B., J. Morton, and K. Mauersberger (1990), Measurement of isotopic abundances in collected stratospheric ozone samples, *Geophys. Res. Lett.*, *17*, 1295–1298.

Sparks, R. K., L. R. Carlson, K. Shobatake, M. L. Kowalczyk, and Y. T. Lee (1980), Ozone photolysis—Determination of the electronic and vibrational-state distributions of primary products, *J. Chem. Phys.*, *72*, 1401–1402.

Taherian, M. R., and T. G. Slanger (1985), Products and yields from O_3 photodissociation at 1576-Å, *J. Chem. Phys.*, *83*, 6246–6250.

Thiemens, M. H., and J. E. Heidenreich (1983), The mass-independent fractionation of oxygen—A novel isotope effect and its possible cosmochemical implications, *Science*, *219*, 1073–1075.

Thiemens, M. H., and T. Jackson (1988), New experimental-evidence for the mechanism for production of isotopically heavy O_3, *Geophys. Res. Lett.*, *15*, 639–642.

Turnipseed, A. A., G. L. Vaghjiani, T. Gierczak, J. E. Thompson, and A. R. Ravishankara (1991), The photochemistry of ozone at 193 and 222 nm, *J. Chem. Phys.*, *95*, 3244–3251.

Wine, P. H., and A. R. Ravishankara (1982), O_3 photolysis at 248 nm and $O(^1D_2)$ quenching by H_2O, CH_4, H_2, and N_2O: $O(^3P_J)$ yields, *Chem. Phys.*, *69*, 365–373.

Yoshino, K., D. E. Freeman, J. R. Esmond, and W. H. Parkinson (1988), Absolute absorption cross-section measurements of ozone in the wavelength region 238–335 nm and the temperature-dependence, *Planet. Space Sci.*, *36*, 395–398.

Yoshino, K., J. R. Esmond, D. E. Freeman, and W. H. Parkinson (1993), Measurements of absolute absorption cross-sections of ozone in the 185-nm to 254-nm wavelength region and the temperature-dependence, *J. Geophys. Res.*, *98*, 5205–5211.

Yung, Y. L., and C. E. Miller (1997), Isotopic fractionation of stratospheric nitrous oxide, *Science*, *278*, 1778–1780.

Yung, Y. L., J. S. Wen, J. P. Pinto, M. Allen, K. K. Pierce, and S. Paulson (1988), HDO in the Martian atmosphere—Implications for the abundance of crustal water, *Icarus*, *76*, 146–159.

Yung, Y. L., W. B. Demore, and J. P. Pinto (1991), Isotopic exchange between carbon dioxide and ozone via $O(^1D)$ in the stratosphere, *Geophys. Res. Lett.*, *18*, 13–16.

Yung, Y. L., A. Y. T. Lee, F. W. Irion, W. B. DeMore, and J. Wen (1997), Carbon dioxide in the atmosphere: Isotopic exchange with ozone and its use as a tracer in the middle atmosphere, *J. Geophys. Res.*, *102*, 10,857–10,866.

G. A. Blake, M. C. Liang, J. D. Weibel, and Y. L. Yung, Division of Geological and Planetary Sciences, California Institute of Technology, MS150-21, 1200 E. California Boulevard, Pasadena, CA 91125, USA. (gab@gps.caltech.edu; mcl@gps.caltech.edu; weibel@gps.caltech.edu)

F. W. Irion, Jet Propulsion Laboratory, Pasadena, CA 91109, USA. (bill.irion@jpl.nasa.gov)

C. E. Miller, Atmospheric Chemistry Element, Jet Propulsion Laboratory, Pasadena, CA 91109, USA. (charles.e.miller@jpl.nasa.gov)